

UDC 536.24.01

*В роботі приведені результати експериментального дослідження теплофізичних властивостей холодильного мінерального компресорного мастила (ISO 9) з домішками наночастинок MoS<sub>2</sub> (70 нм) і Cu (50 нм), а також результати вимірів тиску насиченої пари сумішей ізобутану з отриманими наномастилами. Отримані результати демонструють позитивний вплив домішок наночастинок на характеристики робочих тіл холодильних апаратів*

*Ключеві слова: розчин холодоагент/мастило, теплофізичні властивості, тиск насиченої пари, наночастинка, наномастило*

*В работе представлены результаты экспериментального исследования теплофизических свойств холодильного минерального компрессорного масла (ISO 9) с примесями наночастиц MoS<sub>2</sub> (70 нм) и Cu (50 нм), а также результаты измерений давления насыщенных паров смесей изобутана с полученными наномаслами. Полученные результаты демонстрируют положительное влияние примесей наночастиц на характеристики рабочих тел холодильных аппаратов*

*Ключевые слова: раствор хладагент/масло, теплофизические свойства, давление насыщенных паров, наночастица, наномасло*

# SURFACE TENSION, VISCOSITY, AND THERMAL CONDUCTIVITY OF NANOLUBRICANTS AND VAPOR PRESSURE OF REFRIGERANT / NANOLUBRICANT MIXTURES

**D. Nikitin**

Docent

Department of Programming\*

**V. Zhelezny**

Professor\*\*

E-mail: vzhelezny@mail.ru

Contact tel.: +38 (048) 268-23-39

**V. Grushko**

Graduate Student\*\*

E-mail: vadimgrushko88@gmail.com

Contact tel.: +38 (093) 755-75-88

**D. Ivchenko**

Graduate Student\*\*

E-mail: dmitriy.ivchenko@gmail.com

Contact tel.: +38 (066) 041-50-35

\*\*Department of Engineering Thermophysics

\*Odessa National Academy of Food Technologies

Dvoryanska Str, 1/3, Odessa, Ukraine, 65082

## 1. Introduction

Nanofluids represent colloidal suspensions with particles size of up to 100 nm in the underlying fluid. Impurity of nanoparticles in the liquid could lead to the significant increase in thermal conductivity and vapor pressure, intensify the boiling heat transfer, could reduce friction and, therefore, the wear of mating parts of mechanisms. Currently, inclusion of nanoparticles to the composition of compressor working fluids could be considered as one of the most promising methods for improving refrigeration performance [1, 2]. Most often, nanoparticles are added to the compressor lubricant that is the essential component of refrigeration real working fluid (RWF) [3]. At the same time increase of energy efficiency of refrigeration equipment could be achieved by changes in RWF thermophysical properties, reduce of friction in the mating parts of compressor systems, and enhancement of heat transfer in evaporator. In turn, increase of heat transfer coefficient in the evaporator

depends not only on refrigerant thermophysical properties changes, but also on the formation of additional centers of vaporization [4]. Stability of nanofluids essentially determines the prospect of their use in refrigeration and a key challenge in studying their properties. Clustering facilitates nanoparticles fusion, which causes precipitation in the studied nanofluids. This effect leads to the change of nanofluid concentration. Changing of nanolubricant composition should be reflected in the dynamics of changes in the nanofluid thermophysical properties. These circumstances make nanorefrigerants applications in refrigeration systems quite problematic. In order to study these problems, the measurements of surface tension, viscosity, and thermal conductivity of nanolubricants and also of vapor pressure for the refrigerant/nanolubricant mixtures were provided. The composition of the investigated substances was consisted of the following components: nanopowder - TiO<sub>2</sub> (10 nm), MoS<sub>2</sub> (70 nm), and Cu (50 nm), mineral compressor oil ISO 9, and refrigerant R600a. A choice of surface tension

as one of the properties under investigation was dictated by the fact that any clustering process will lead to a change in the composition of the surface layer of the nanolubricant liquid phase. Thus, possible changes in surface tension of the nanolubricant and, hence, of the saturated vapor pressure [5] of the nanolubricant/refrigerant mixture is a reliable indicator reflecting the stability of working fluids in the refrigeration equipment.

## 2. Samples preparation

Analysis of published works devoted to the study of thermophysical properties of nanofluids [1, 2] shows that the sample preparation is perhaps the key factor for obtaining stable over time nanofluids. Techniques of uniform dispersion of nanoparticles in the liquid is a prerequisite for obtaining high-quality and most importantly, reproducible results of the experimental data.

In our research, a special attention was done to the sample preparation to provide their stability over the time. Characteristics of the original oil sample and nanoparticles TiO<sub>2</sub> are given in Tables 1 and 2. The average size of nanoparticles in the oil was determined by dynamic light scattering (laser spectroscopy correlation).

Characteristics of the compressor mineral oil ISO 9

Density at 20°C, kg/m <sup>3</sup>	Kinematic viscosity at 40°C, cSt	Kinematic viscosity at 100°C, cSt	Acid number	Flash Point, K	Pour Point, K	Pseudo critical temperature, K	Pseudo critical pressure, MPa
877	10.7	2.68	0.02	426	223	767*	1.20*

*\*) A part of the oil properties were obtained in the Odessa State Academy of Refrigeration and from the oil manufacturer, the pseudo-critical parameters were obtained by the pulse method at the Institute of Thermal Physics, Ural Scientific Center, Russian Academy of Sciences [6].*

Table 2

Specifications of the nanoparticles TiO<sub>2</sub>

Color	Composition of the nanoparticles		Specific surface of the nanoparticles	Average particle size
	Rutile, %	Anatase, %		
Light-gray	28	72	49 m <sup>2</sup> /g	10 nm

Initial concentration of the TiO<sub>2</sub> nanoparticles in oil was vol. 10%. The sample was diluted with the pure oil to the concentration of 5% and then was stirred by the electromagnetic stirrer during several hours. The obtained sample had a significantly lower viscosity, allowing preparing the working samples of nanolubricants with different concentrations. The mass concentration of nanoparticles was calculated by the formula

$$C = \frac{\rho_{TiO_2} \cdot (\rho_{nf} - \rho_A)}{\rho_{nf} (\rho_{TiO_2} - \rho_A)} \cdot 100, \quad (1)$$

here  $\rho_{TiO_2}$  = density of nanoparticles,  $\rho_{nf}$  = density of nanofluid,  $\rho_A$  = density of oil.

The mass concentration of the prepared sample was 0.008%. To destruct agglomerations of nanoparticles, a sample was homogenized by using ultrasonic disperser at room temperature for 30 minutes. To separate nanoparticle clusters, the sample was centrifuged for 45 minutes. Thus the mixture became transparent, homogeneous and could be used for further investigations. Hydrodynamic radius of TiO<sub>2</sub> nanoparticles in oil was measured with laser correlation spectroscopy method that is also known as the dynamic light scattering technique. It was 10 nm with an uncertainty of 5%. Preparation of nanofluids based on oil and MoS<sub>2</sub> and Cu nanoparticles was completed by gravimetric method, followed by stirring the sample by the electromagnetic stirrer and an ultrasonic disperser and centrifugation. The concentration of MoS<sub>2</sub> and Cu nanoparticles in the oil was equal to 0.1%.

## 3. Experimental research

### 3.1. Surface Tension

Table 1

The Maximum Bubble Pressure method [8] was used to study the nanolubricant surface tension. The advantages of this method are relatively low uncertainty of the obtained experimental data and lack of the contact angle magnitude in the calculation formulas (its value can be changed by adding nanoparticles into the liquid) [8]. The experimental setup is shown in Figure 1. The main element of the setup is the calibrated capillary tube located in the measuring cell. The inner diameter of the capillary tube (in the bottom part) was equal to 0.86 mm. The upper end of the capillary is connected to the atmosphere. The outer casing of the measuring cell is a pumped thermostat through which the chiller liquid is circulated. Internal volume of the measuring cell is filled with test liquid so that the capillary was immersed in a liquid to a depth of not less than 15mm. Immersion depth of the capillary into the liquid was measured by the cathetometer with the uncertainty of 0.02 mm.

The top of the capillary has a damper extension to reduce the pressure pulsations in creating vacuum in the internal volume of the measuring cell. With open drip, the liquid with low vapor pressure follows from the measuring vessel to the glass, creating a vacuum in the internal volume of the measuring cell. By adjusting the frequency separation of drops, one can create the necessary negative pressure in the internal volume of the measuring cell, required for the formation of air bubble at the end of the capillary in the liquid. Maximum pressure in the bubble is fixed by the differential pressure gauge. The upper part of the measuring cell is a hermetically closed tube. A copper-constantan thermocouple connected to a temperature measuring device is installed inside the measuring cell.

Surface tension was calculated as

$$\sigma = \frac{R}{2} \cdot \rho_m \cdot g \cdot H_{max} \cdot K, \quad (2)$$

here  $R$  = internal capillary radius;  $\rho_m$  = density of the manometric fluid;  $g$  is gravity acceleration;  $K$  = coefficient accounted for type of manometric fluid;  $H_{max}$  = maximum lifting height of the manometric fluid.

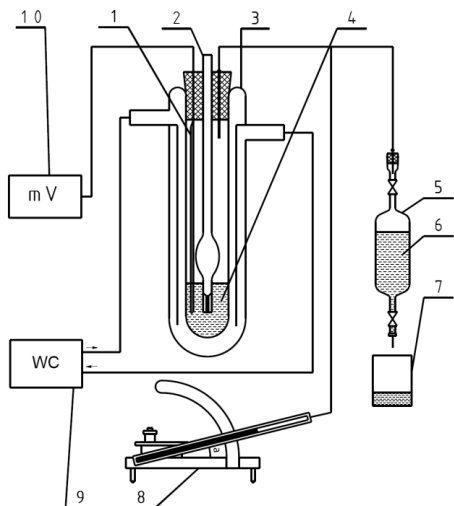


Fig. 1. Surface tension measuring device: 1 - thermocouple; 2 - calibrated capillary tube; 3 - measuring cell; 4 - nanofluid; 5 - graduated vessel; 6 - oil; 7 - glass; 8 - micromanometer; 9 - water cooler; 10 - millivoltmeter

### 3.2. Saturated Vapor Pressure

Saturated vapor pressure (VLE) measuring device using the Static method is shown in fig. 2. The main part of the measuring device is a constant volume cell with the ballast capillary tube. The volume of the cell is equal to 346.49  $sm^3$ . The cell is placed into the temperature bath, and experimental temperature was measured by the thermometer with the uncertainty of 0.1 K.

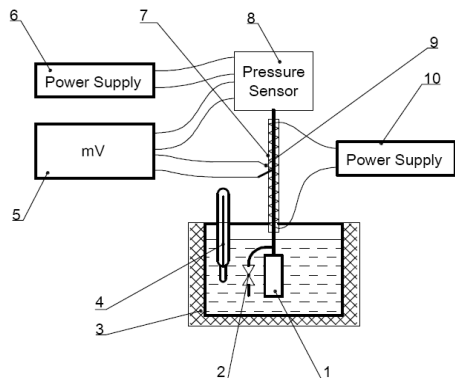


Fig. 2. VLE measuring device: 1 - measuring cell; 2 - hot valve; 3 - thermostat; 4 - thermometer; 5 - millivoltmeter; 6, 10 - power supplies; 7 - heater; 8 - pressure sensor; 9 - thermocouple.

A piezoelectric pressure transducer, attached to the top of the ballast capillary is used for the vapor pressure measurements. Special design heater prevents possibility

of the refrigerant condensation on the ballast capillary. The temperature of the capillary was measured by the thermocouple connected to the sensitive millivoltmeter. Before charging the measuring cell, the samples of the fluid under investigation (oil/refrigerant mixture with nanoparticles) were purified from the dissolved air. The concentration of the mixture components was performed by gravimetric method. The criteria for establishing thermodynamic equilibrium in the measuring cell are the stable reading of temperature and saturated vapor pressure in the measuring cell. An uncertainty of the experimental results did not exceed 1%.

### 3.3. Thermal Conductivity

Thermal conductivity was measured using the Modified Steady-State Hot-Wire method. The construction of the measuring cell and thermal conductivity measuring device are shown in fig. 3. A special feature of this apparatus is the application of a thin-walled platinum capillary tube (outer diameter = 1.0 mm, inner diameter = 0.9 mm) as the outer resistance thermometer. A platinum wire (diameter = 0.1 mm and length = 80 mm) located inside this capillary tube is used as an electric heater and at the same time as the inner resistance thermometer. In order to center this wire inside the capillary tube, the latter was placed within a glass tube that can be adjusted in two orthogonal directions by set screws. The wire was centered by visual observation using a microscope. The frame for this apparatus was designed to have minimal clearance with the glass tube, thus eliminating convective heat transfer from the tube outside.

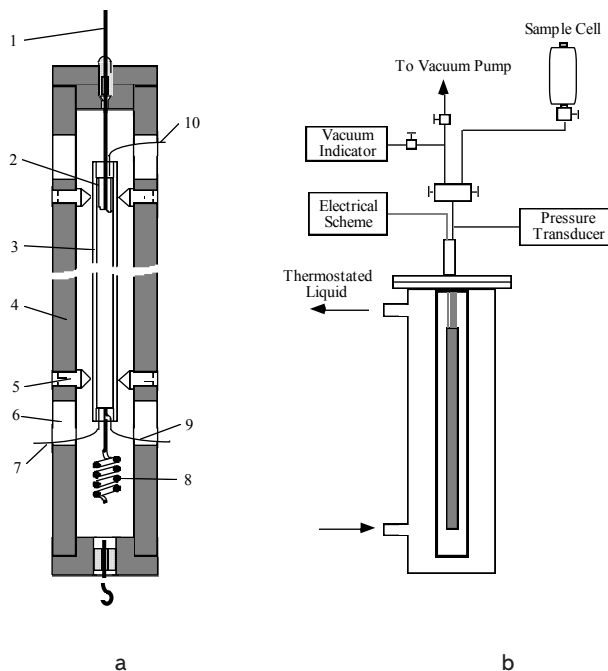


Fig. 3. Thermal conductivity apparatus. a) Measuring cell: 1 - central wire; 2 - platinum capillary; 3 - glass capillary; 4 - frame; 5 - set screw; 6 - window for visual observation; 7 - potential connection to capillary; 8 - spring; 9 - potential connection to wire; 10 - current connection to capillary. b) Thermal conductivity measuring device

Thermal conductivity was calculated from the measured temperature difference, current, and resistance using the formula

$$\lambda = \frac{\ln\left(\frac{d_2}{d_1}\right) I^2 \cdot R}{2 \cdot \pi \cdot l \cdot \Delta T}, \quad (3)$$

here  $d_2$  = inner diameter of platinum capillary tube,  $d_1$ =diameter of platinum wire,  $l$ =length of this wire,  $I$ =current,  $R$  = resistance of the wire,  $\Delta T$  = temperature difference between the wire and the capillary tube.

The geometric constant of the measuring cell,  $\ln(d_2/d_1)/2 \cdot \pi \cdot l$ , was determined by measuring the values of  $d_1$ ,  $d_2$ , and  $l$ , and then was verified by experiments using standard reference data for toluene. Thermal conductivity was calculated taking into account the corrections for end effects, eccentricity of the wire, and radiation heat transfer. The sum of these corrections did not exceed 0.5% of the measured thermal conductivity.

The apparatus was installed in the vessel (fig. 3b), placed in the special constant temperature bath to provide temperature control within  $\pm 0.01$  K. The temperatures of both resistance thermometers were determined by measuring the potential difference across each thermometer relative to the potential across standard resistances. The accuracy of these measurements using a digital voltmeter is within  $\pm 10$  nV. During thermal conductivity measurements, the temperature drop between the wire and the capillary tube in the fluid sample was 4 – 10 K. For these conditions,  $Ra = Gr \cdot Pr$  values were less than 1000 in all experiments, indicating negligible natural convection effects. Calculated uncertainties in the experimental thermal conductivities were within  $\pm 0.8\%$ .

### 3.4. Viscosity

Kinematic viscosity was measured by the Capillary Tube Method (glass viscometer with, so called, “hanging level”). Two capillary tubes with diameters 0.82 and 1.12 mm were used. Viscosity was calculated by the formula

$$\nu = \frac{g}{9.807} \cdot t \cdot K, \quad (4)$$

where  $\nu$  = kinematic viscosity,  $g$  = local acceleration due to gravity,  $t$  = average flow time,  $K$  = viscometer constant.

The viscometer was installed in the glass Dewar vessel, and the temperature of this vessel was controlled within  $\pm 0.02$  K. Calculated uncertainties in the experimental viscosity data did not exceed  $\pm 0.5\%$ .

## 4. Results and discussion

The temperature dependence of the surface tension of the pure mineral oil and the oil with the  $\text{MoS}_2$  and  $\text{TiO}_2$  nanoparticles is shown in the fig. 4, and the results of saturated vapor pressure measurements for the R600a/oil mixture with the  $\text{TiO}_2$  nanoparticles are given in the fig. 5.

As it is seen from the fig. 4, the influence of the nanoparticles on the surface tension is valuable (up to 12%)

despite of the small concentration of  $\text{TiO}_2$ . This fact may have a positive impact on the performance of the compression systems (decrease of the oil surface tension should lead to increase of vapor pressure of the refrigeration working fluid in the crankcase, as it is seen from the fig. 5). The growth of vapor pressure of the nanorefrigerant will increase its density. Consequently, the mass flow of refrigerant and the cooling capacity of the compressor system have to increase.

Analysis of the obtained experimental phase equilibrium data shows that the influence of nanoparticles on the vapor pressure depends on the temperature (see fig. 6 and 7). For the system R600a/oil +  $\text{TiO}_2$ , this influence increases with increasing of the temperature. Opposing, for the system R600a/oil +  $\text{MoS}_2$ , the reverse effect is observed. The effect of nanoparticles on the saturation vapor pressure decreases with increasing the temperature. The greatest contribution of nanoparticles to the vapor pressure is observed at the mass oil concentration equal to 0.3. These effects probably related to the different influence of nanoparticles on the structure of the surface layer of the liquid phase of the refrigerant/oil mixture.

The structure of the surface layer of the nanofluid liquid phase is determined by the nature of diffusion processes at the liquid-vapor interface. These processes, in turn, depend on the ratio of nanoparticles and oil densities, viscosity, and thermodynamic parameters.

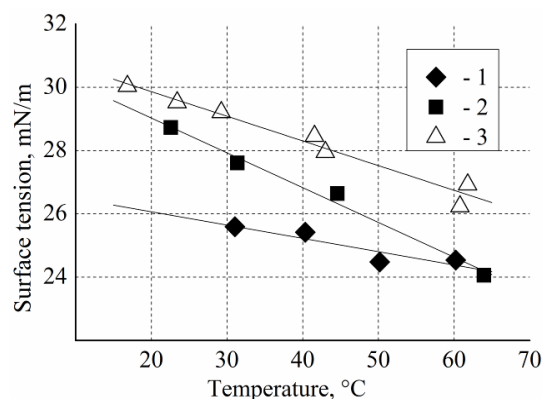


Fig. 4. Surface tension of pure oil (1), oil with  $\text{MoS}_2$  (2), and oil with  $\text{TiO}_2$  (3)

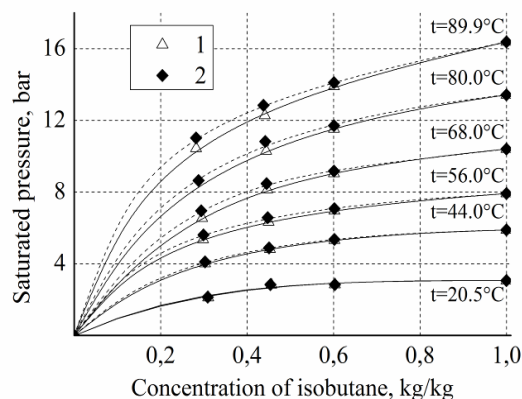


Fig. 5. Saturated vapor pressure of R600a/oil (1) and R600a/oil with  $\text{TiO}_2$  (2)

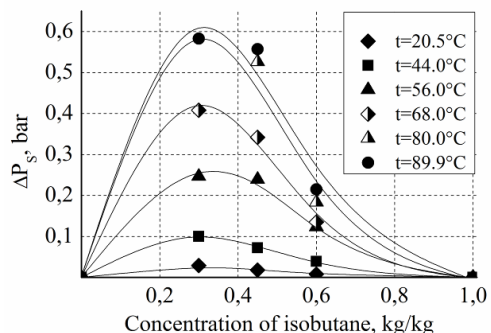


Fig. 6. Deviations in saturated pressures of mixture R600a/oil and R600a/Azmol + TiO<sub>2</sub>

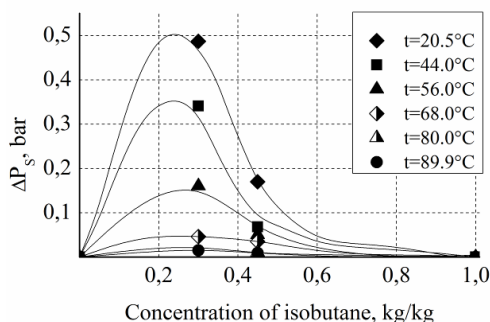


Fig. 7. Deviations in saturated pressures of mixture R600a/oil and R600a/Azmol + MoS<sub>2</sub>

The influence of the TiO<sub>2</sub> and Cu nanoparticles on the thermal conductivity and viscosity of the compressor oil (our experimental data) is show in the fig. 8.

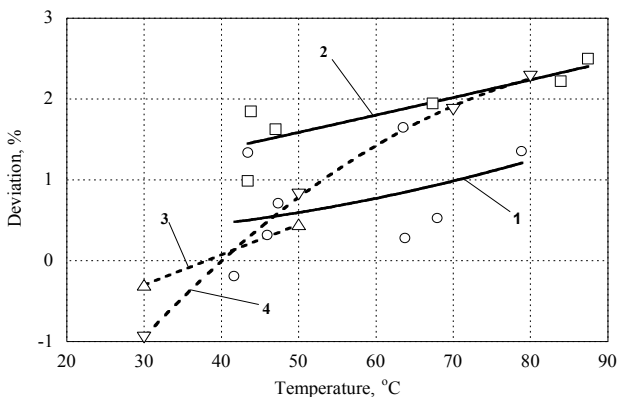


Fig. 8. Deviations of experimental transport property data for mineral oil with nanoparticles from the data for pure oil: 1 - thermal conductivity of oil + TiO<sub>2</sub>; 2 - thermal conductivity of oil + Cu; 3 - viscosity of oil + TiO<sub>2</sub>; 4 - viscosity of oil + Cu

The measurements were done at very small nanoparticle concentrations (0.008% and 0.1%, consequently). These concentrations values were chosen because of the specific compressor refrigeration system, since the loss of nanoparticles in the sediment could effect the operation of the throttle device. As it is seen from the fig. 8, the established effect is not high but it could be augmented at higher nanoparticle concentrations or with another type of nanoparticles. Further researches of the transport properties are required.

### 5. Conclusions

Methodology of preparation of the nanofluids consisted of refrigeration compressor lubricant (mineral oil ISO 9) with nanoparticles of TiO<sub>2</sub> (10 nm), MoS<sub>2</sub> (70 nm), and Cu (50 nm) is described. A set of experimental devices and procedure of measuring thermophysical properties (surface tension, saturated vapor pressure, thermal conductivity, and viscosity) are given, the experimental data for the surface tension, thermal conductivity, and viscosity of the mineral oil with the nanoparticles of TiO<sub>2</sub>, MoS<sub>2</sub>, and Cu, and also for the saturated vapor pressure of the R600a/oil mixture with the TiO<sub>2</sub> nanoparticles are obtained. The experimental results are discussed. Our research shows that small admixtures of nanoparticles in the compressor oil in a large extent affect the surface properties of liquids (surface tension and saturated vapor pressure). A positive impact of nanoparticles on the performance of compressor systems is considered. It is shown that further research on influence of temperature, shape, nature and concentration of nanoparticles, and also the nature of the solvent are needed.

### References

1. Analysis of the prospects of using of nanofluids in the refrigeration systems. Part 1: Thermophysical properties of nanofluids / V.P. Zhelezny, B.V. Kosoy, S.S. Krijanovsky, E.S. Obolonsky, Ravi Kumar: *Trudy. «Obladnannya ta Tehnologii Harchovih Virobnictv»* (Proc. "Equipment and Technologies for Food Production"). — Doneck, 2009. — 21. — p. 329–340.
2. Analysis of the prospects of using of nanofluids in the refrigeration systems. Part 2 / V.P. Zhelezny, B.V. Kosoy, S.S. Krijanovsky, E.S. Obolonsky, Ravi Kumar: *Trudy. «Obladnannya ta Tehnologii Harchovih Virobnictv»* (Proc. "Equipment and Technologies for Food Production"). — Doneck, 2009. — 21. — p. 341–351.
3. Zhelezny, V.P. Influence of compressor oil admixtures on efficiency of a compressor system / V.P. Zhelezny, S.V. Nichenko, Yu.V. Semenyuk, B.V. Kosoy, Ravi Kumar // *Int. J. Refrig.*— 2009.— 32(7). — p. 1526–1535.
4. Effect of CuO nanoparticle concentration on R134a-lubricant pool boiling heat transfer / M. A. Kedzierski: *Proceedings Micro-Nanoscale Heat Transfer International Conference.* — Taiwan, 2008. — N. Y. — p. 1–8.
5. Technique for forecasting liquid surface tension from the data on saturated vapor pressure / Yu.V. Semenyuk, D.A. Ivchenko, V.P. Zhelezny, *Trudy. «Obladnannya ta Tehnologii Harchovih Virobnictv»* (Proc. "Equipment and Technologies for Food Production"). — Doneck, 2010. — 24. — p. 17–25.
6. Skripov, P.V. Comparison of thermophysical properties for oil/refrigerant mixtures by use the pulse heating method / P.V. Skripov, A.A. Starostin, D.V. Volosnikov, V.P. Zhelezny // *Int. J. Refrig.*— 2003. — 26. — p. 721–728.
7. Thermodynamic and thermophysical behavior of the suspension of uranium dioxide / J.S. Takibaev, G.C. Potrebnikov, N.N. Pavlova, A.B. Lotov: *NNC RK Bulletin* 2005. — 1(21). — p. 38–45.
8. Adamson, A.W. *The physical chemistry of surfaces* / A.W. Adamson. — New York: Wiley, 1976. — 698 p.

**Abstract**

The results of thermophysical property and vapor-liquid equilibria studies for the systems mineral oil ISO 9 + MoS<sub>2</sub> (70 nm) and Cu (50 nm) nanoparticles, and R600a + nanolubricant are presented. Series of measurements: surface tension (maximum bubble pressure method), thermal conductivity (steady-state hot-wire method), viscosity (capillary tube method), and saturated vapor pressure (static method) were carried out. The size and the concentration of nanoparticles in the lubricant were determined by dynamic light scattering (laser correlation spectroscopy). Experimental data demonstrate some positive effect of nanoparticles doping on the refrigerant properties such as the decreasing of nanolubricant surface tension, thermal conductivity growth, and the shift of vapor pressure curve in refrigerant/lubricant blends. Thus, the use of nanorefrigerants shows clearly the energy efficiency enhance for the vapor compression refrigerating systems

**Keywords:** refrigerant/lubricant mixture, thermophysical properties, saturated vapor pressure, nanoparticles, nanolubricant

УДК 616-71

# МАТЕМАТИЧНА МОДЕЛЬ НАГРІВАННЯ БІОЛОГІЧНИХ ТКАНИН ПІД ДІЄЮ ЛАЗЕРНОГО ВИПРОМІНЮВАННЯ

Ми представляємо математичну модель нагрівання біологічних тканин під дією лазерного випромінювання, яка надає змогу оцінити розподіл температури в біологічних тканинах під дією лазерного випромінювання

**Ключові слова:** розподіл температур, лазерне випромінювання, напівпрозоре середовище

Мы представляем математическую модель нагрева биологических тканей под действием лазерного излучения, которая предоставляет возможность оценить распределение температуры в биологических тканях под действием лазерного излучения

**Ключевые слова:** распределение температур, лазерное излучение, полупрозрачная среда

**О.Д. Мамута**  
Аспірант\*

Контактний тел.: (044)454-96-09, 093-071-96-60  
E-mail: mamuta\_aleksandr@mail.ru

**М.С. Рибалко**  
Аспірант\*

Контактний тел.: (044)454-94-77  
E-mail: RybalkoMaryna@gmail.com

**Л.Ф. Головко**

Доктор технічних наук, професор  
Контактний тел.: (044) 454-96-09  
E-mail: leongolovko@gmail.com

\*Кафедра лазерної техніки та фізико-технічних технологій  
Національний технічний університет України  
«Київський політехнічний інститут»  
пр. Перемоги, 37, м. Київ, Україна, 03056

## Вступ

Лазерне випромінювання впливає на біологічну тканину такими фізичними факторами як температура, слабкий електричний струм, тиск та ін. Відмінною особливістю його впливу є локалізація. Хвилі світлового діапазону випромінювання поглинаються та відбиваються поверхнею біотканини, промені височастотні проникають глибше, але в будь-якому випадку зона впливу охоплює тільки частину біологічної тканини. Існують різні підходи до розв'язання задачі впливу лазерного випромінювання на біологічну тка-

нину та безліч різноманітних фізичних і числових моделей. Відомі з літературних джерел моделі взаємодії біотканини з лазерним випромінюванням об'єднують такі їх особливості:

1. Кожний шар має свої незалежні фізичні властивості.
2. Має місце складна або випадкова геометрія шарів біологічних тканин.
3. Необхідність врахування перфузії крові, що пов'язана з кровеносними судинами у живій біологічній тканині, які здійснюють терморегуляцію в організмі.